Tetrahedron 67 (2011) 7348–7353

Contents lists available at ScienceDirect

Tetrahedron

journal homepage: www.elsevier.com/locate/tet

A rapid responsive and highly selective probe for cyanide in the aqueous environment

Hongda Li [a], Bao Li [b], Long-Yi Jin [a], Yuhe Kan [c,*], Bingzhu Yin [a,*]

[a] Key Laboratory of Natural Resources of Changbai Mountain & Functional Molecules, Yanbian University, Ministry of Education, Yanji, Jilin 133002, PR China
[b] State Key Laboratory of Supramolecular Structure and Materials, College of Chemistry, Jilin University, Changchun 130012, PR China
[c] Jiangsu Key Laboratory for Chemistry of Low-Dimensional Materials, Huaiyin Teachers College, Huaiyin 223300, PR China

ARTICLE INFO

Article history:
Received 9 May 2011
Received in revised form 8 July 2011
Accepted 12 July 2011
Available online 20 July 2011

Keywords:
Trifluoroacetaminocoumarin
Fluorescent probe
Cyanide detection
DFT/TDDFT calculation
ICT

ABSTRACT

A colorimetric and fluorescent cyanide probe based on 7-(trifluoroacetamino)coumarin has been prepared. This structurally simple probe displays rapid response and high selectivity for cyanide over other common anions in the aqueous solution. The sensing of cyanide was performed via the nucleophilic attack of cyanide anion to carbonyl of the probe with a 1:1 binding stoichiometry, which could be confirmed by Job's plot, ^{1}H NMR, and MS studies. DFT/TDDFT calculations support that the fluorescence enhancement of the probe is mainly due to the ICT process improvement. The detection limit of the fluorescent assay for cyanide is as low as 0.3 μM in a rapid response of less than 30 s. Thus, the present probe should be applicable as a practical system for the monitoring of cyanide concentrations in aqueous samples.

1. Introduction

Cyanide is well known one of the most toxic materials and extremely harmful to the environment and human health.[1] Nevertheless, a large amount of cyanides are extensively utilized in different fields, such as gold mining, electroplating, metallurgy, synthetic fibers, and resins industry. The extreme toxicity of cyanide ions in physiological[1–3] as well as environmental[4] systems has led many researchers to develop optical probes[5,6] for the sensitive and selective detection of cyanide. Up to date, several strategies have been developed to detect cyanide, including the formation of cyanide complexes with transition metals,[7–11] boron derivatives,[12,13] and CdSe quantum dots,[14,15] the displacement approach,[16] hydrogen-bonding interactions,[17–19] deprotonation,[20] and luminescence lifetime measurement.[21] In order to minimize the interferences of other anions, the nucleophilic addition reactions of cyanide were applied for sensing of cyanide, including reactions with oxazine,[22–24] pyrylium,[25] squarane,[26] acyltriazene,[16] acridinium,[27] salicylaldehyde,[28–30] trifluoroacetophenone,[31–35] trifluoroacetamide derivatives,[36–40] and other highly electron-deficient carbonyl groups or imine.[19,41–45] Although the nucleophilic addition reactions of cyanide demonstrated good sensitivity and selectivity for cyanide, the practical detection of cyanide involves certain inherent disadvantages, such as poor selectivity over fluoride or acetate, not instantaneously registering the addition of cyanide and complicated synthesis. In addition, many of them are reported to work only in organic media, so the search for effective sensing systems in aqueous environment is still a great challenge. Very recently, an indole conjugated coumarin chemodosimeter with a rapid response time (<1.0 s) was reported, but which is short of experimental data to confirm the response time.[46]

Keeping above-mentioned information in mind, we wish to report a novel colorimetric and fluorescent cyanide probe **1** bearing a trifluoroacetamide functionality for highly selective cyanide detection in aqueous environment (Scheme 1). Probe **1** is designed on the basis of trifluoroacetyl binding element and 7-amino-4-trifluoromethylcoumarin fluorophore, which were connected by an amide unit. Cyanide is expected to be detectable by nucleophilic attack toward a highly electron-deficient carbonyl group of **1**, which is activated by two trifluoromethyl and a lactone group.[20]

2. Results and discussion

2.1. Synthesis and crystal structure analysis

Probe **1** was synthesized in one-step as outlined in Scheme 1. The reaction of 7-amino-4-trifluoromethylcoumarin with trifluoroacetic anhydride gave probe **1** in good yield in the THF at

* Corresponding authors. Tel.: +86 433 2732298; fax: +86 433 2732456; e-mail address: zqcong@ybu.edu.cn (B. Yin).

0040-4020/$ – see front matter Crown Copyright © 2011 Published by Elsevier Ltd. All rights reserved.
doi:10.1016/j.tet.2011.07.023

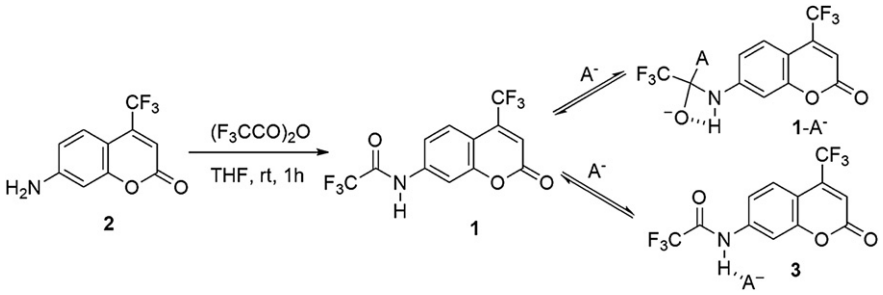

Scheme 1. Synthetic procedure and proposed cyanide-sensing mechanism of probe **1**.

room temperature. Probe **1** has been characterized by ^{1}H NMR, ^{13}C NMR, MALDI-TOF MS, and elemental analysis. The structure of probe **1** was further confirmed by X-ray crystallography. White crystals suitable for an X-ray diffraction study were obtained by slowly evaporating a benzene solution of probe **1** at room temperature. Single-crystal X-ray diffraction structure analysis indicates that probe **1** crystallizes in triclinic system, P−1 space group. The asymmetric unit consists of one whole molecule, as shown in Fig. 1. In the crystal structure of probe **1**, the whole molecule is approximately coplanar with the mean deviation is 0.0501 (2) Å except F atoms. The F atoms link to C12 express a positional disordered with the ratio of site occupations 0.525:0.475, while the other three F atoms do not show the similar conditions. The adjacent molecules are connected each by intermolecular N—H···O and N—H···O hydrogen bonds, forming one-dimensional chains along [210] direction. A summary of the crystallographic data and structural refinements for probe **1** and the hydrogen-bonding interactions in probe **1** are listed in Table S1 and S2 (see Supplementary data).

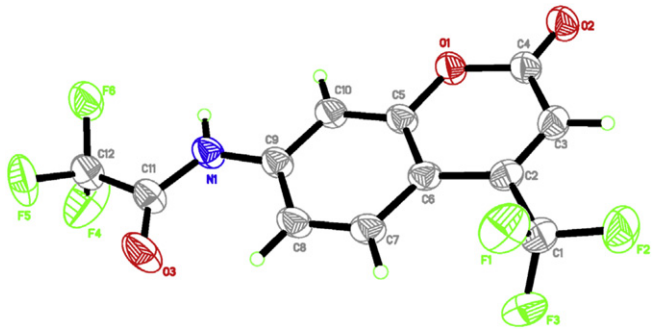

Fig. 1. The single crystal X-ray structure of probe **1**.

2.2. The binding affinity and selectivity of probe 1 for anions

Considering a report in the literature,[34] the present probe **1** would interact with anions by reversible covalent bonding to form adduct **1**-A^- and less efficiently by direct H-bonding to form species **3** (Scheme 1). Upon anion binding on its trifluoroacetamide receptor in probe **1**, the degree of ICT is expected to be dependent less on the anion's H-bonding ability but may be dependent on the anion's carbonyl carbon affinity; hence, the usual guest selectivity pattern dependent on the anion's H-bonding ability and/or basicity may be altered. An anion, that is, a weak H-bonding acceptor but has strong carbonyl carbon affinity is expected to be differentiated from other anions that are strong H-bonding acceptors, particularly in aqueous media, because weak solvation is expected in the former case. Indeed, when probe **1** was treated with selected anions, such as CN^-, F^-, CH_3COO^-, and $H_2PO_4^-$ (50 equiv) in acetonitrile, a new strong peak at 389 nm appeared along with a concomitant decrease at 327 nm. Other anions, such as Cl^-, Br^-, I^-, and HSO_4^- showed diminished absorption change compared to CN^- as seen in Fig. 2a. This result implied that the sensing of cyanide was probably performed via the nucleophilic attack of cyanide anion to carbonyl of the probe **1**, because cyanide is a very weak H-bonding acceptor but has a strong affinity toward the carbonyl carbon. An even more striking feature results when the sensing experiment is carried out in aqueous media. The absorption spectral changes of probe **1** on addition of cyanide in an aqueous solution (acetonitrile/water, 4:1, v/v) are shown in Fig. 2b. The absorption band at 327 nm decreased, while a new red-shifted band at 365 nm appeared. Other competing anions, such as F^-, Cl^-, Br^-, I^-, CH_3COO^-, $H_2PO_4^-$, HSO_4^-, ClO_4^-, NO_3^-, NO_2^- (50 equiv) are completely nonresponsive. No interference of fluoride and acetate anions should arise from their high solvation energies in water as stated above. High solvation energies for F^- (ΔH_{hyd}=−505 kJ/mol) and AcO^- (ΔH_{hyd}=−375 kJ/mol) in water could account for the very weak/negligible binding of probe **1** with both F^- and AcO^- in the present study.[19] The unique affinity of probe **1** toward cyanide over other anions in aqueous media indicates that the competive anions with strong or significant H-bonding ability, such as F^-, AcO^-, and $H_2PO_4^-$ are stabilized by solvation through H-bonding and thus unable to form the corresponding adduct. Only CN^-, which is a poor H-bond acceptor, can add to probe **1** to afford a cyanohydrin, which will be stabilized through intramolecular hydrogen bond between a developed alkoxide anion and an amide proton. The blue shift of absorption of species (from 389 nm to 365 nm) formed by interaction of probe **1** with CN^- in aqueous media compared with that in acetonitrile also supported the nucleophilic addition mechanism as mentioned in Scheme 1.[47] Electronic spectra recorded for probe **1** in CH_3CN/H_2O (4:1, v/v) with increasing CN^- revealed a successive increase in absorption at 365 nm along with a concomitant decrease at 327 nm. These changes were associated with the appearance of three simultaneous isosbestic points at 239, 275, and 341 nm. Simultaneous appearance of isosbestic points signified the presence of two different species that remained in equilibrium. Absorption bands at 327 nm for probe **1** was attributed primarily to the coumarin-based π−π* transition. On binding to the CN^-, the red-shifted and enhanced new band at 365 nm could be attributed to the adduct-based intramolecular charge transfer (ICT) band (Fig. 2c). The variation of the absorbance at 365 nm was used to evaluate the binding constants of **1** with CN^- by assuming a 1:1 binding stoichiometry. The Benesi–Hildebrand[48] analysis of these changes gave a binding constant of 6.67×10^3 M^{-1} (R=0.998). Nice fittings supported the 1:1 binding stoichiometry.[49]

The sensing phenomena were also monitored by fluorescence spectroscopy in CH_3CN/H_2O (4:1, v/v). As cyanide ions were added to probe **1**, the fluorescence emission intensity at 505 nm increased more than 30-fold when excited at 388 nm and was saturated at ca. 50 equiv of cyanide. However, other anions, such as F^-, Cl^-, Br^-, I^-, CH_3COO^-, $H_2PO_4^-$, HSO_4^-, ClO_4^-, NO_3^-, and NO_2^- did not cause any

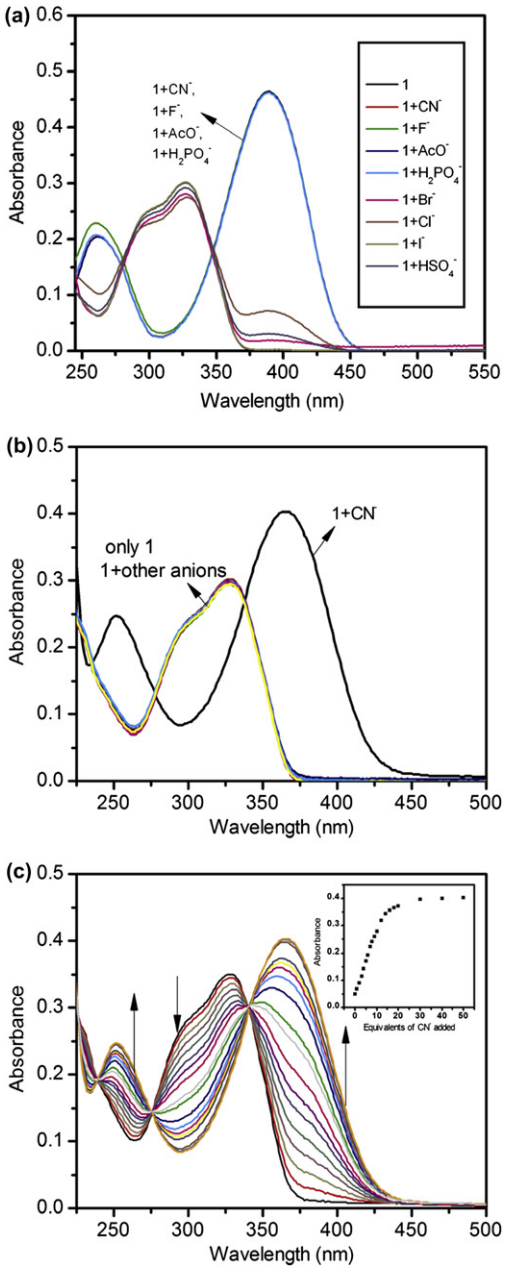

Fig. 2. Absorbance changes of **1** (20 μM) (a) in CH_3CN; (b) in CH_3CN/H_2O (4:1, v/v) upon addition of 50 equiv of various anions (only **1**, CN^-, F^-, Cl^-, Br^-, I^-, AcO^-, ClO_4^-, NO_3^-, $H_2PO_4^-$, NO_2^-, and HSO_4^-); (c) absorption spectra of **1** (20 μM) upon addition of cyanide anion (0–50 equiv). Inset: plots of absorption 365 nm versus the equivalents of CN^- added.

significant changes in the fluorescence emission intensity. The fluorescence profiles at 505 nm showed a high selectivity for cyanide over other various anions (Fig. 3a). A large increase in the fluorescence intensity could be applied to the detection of cyanide anions by the naked eye. When the probe was excited at 365 nm in the presence 50 equiv of other anions in CH_3CN/H_2O (4/1, v/v), a bright blue fluorescence response was selectively observed only in the presence of cyanide in the solution of 20 μM of probe **1** (Fig. 3a, inset). It is well known that starting material **2** (7-amino-4-trifluoromethylcoumarin) is a strong fluorescent molecule.[50] Whereas probe **1** shows very weak fluorescence emission at 505 nm when excited at 388 nm because the internal charge transfer (ICT) from the amino group to the coumarin ring was reduced by an electron-withdrawing trifluoroacetyl group, which induced fluorescence quenching. Conversely, the cyanohydrin formed by addition of cyanide enhanced fluorescence intensity. The fluorescence enhancement is explained by intramolecular H-bonding stabilization of a cyanide adduct, through which an ICT process can be improved. Fig. 3b shows the results of fluorescence titration of probe **1** with CN^-. Job's plot analysis of the fluorescence titration spectra exhibited a maximum at a 0.5 mol fraction of CN^-, indicating formation of a 1:1 adduct between probe **1** and CN^- ion (Fig. 4). On the basis of both the 1:1 stoichiometry and fluorescence titration data from Fig. 3b, the binding constant of probe **1** for CN^- was calculated to be 5.06×10^3 M^{-1} (R=0.999).

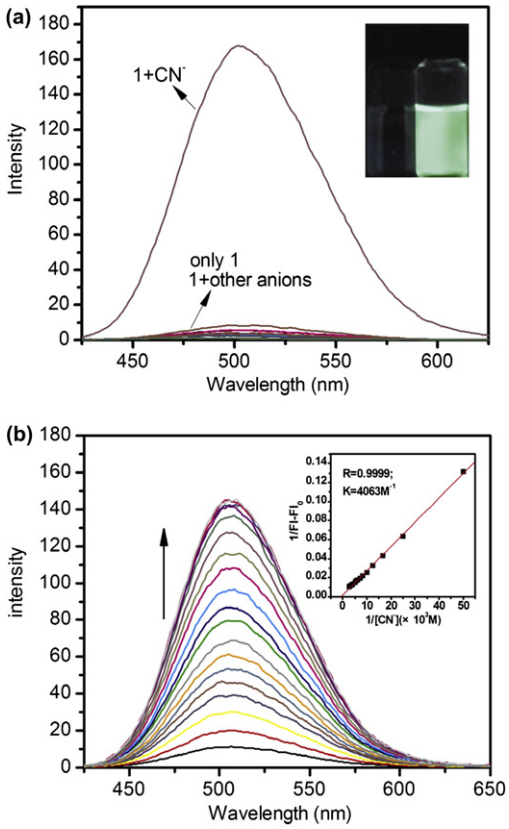

Fig. 3. Fluorescence spectra of **1** (20 μM) (a) upon addition of 50 equiv of various anions. (only 1, CN^-, F^-, Cl^-, Br^-, I^-, AcO^-, ClO_4^-, NO_3^-, $H_2PO_4^-$, NO_2^-, and HSO_4^-), Inset: Fluorescence change observed upon excitation at 365 nm with a laboratory UV lamp after the addition of cyanide anion (50 equiv) to probe **1**; (b) upon addition of cyanide anions (0–80 equiv) in CH_3CN/H_2O (4:1, v/v). The excitation wavelength for the complex was 388 nm, and the splits were 3 nm. Inset: plots of fluorescent emission 505 nm versus the equivalents of CN^- added.

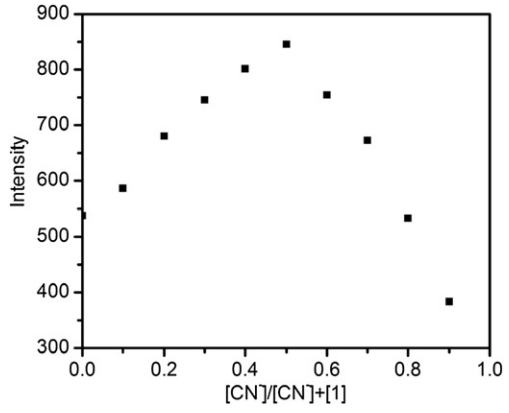

Fig. 4. Job's plot between **1** and cyanide anion. The excitation wavelength for the complex was 388 nm, and the splits were 5 nm; in CH_3CN/H_2O (4:1, v/v) at 25 °C.

To confirm further the interaction mechanism and 1:1 stoichiometry between the cyanide with the probe **1**, ^{1}H NMR titration experiments were carried out by addition of Bu_4NCN to a acetonitrile-d_3 solution of probe **1** (Fig. 5a). With the increasing addition of cyanide, all the aromatic protons exhibited an upfield shift to different extent, which suggest the increase in the electron density in coumarin ring through charge delocalization in the conjugated system.[36–40] However, the absence of any signal for $[H(CN)_2]^-$ does not support the deprotonation phenomena.[19] The spectral shift is virtually stopped after addition of 1 equiv of cyanide. This result also supported the formation of a stable 1:1 adduct. ^{13}C NMR spectral analysis showed that the carbonyl carbon at 155.3 ppm in trifluoroacetyl was highly upfield to 63.4 ppm, while the other aromatic carbons and a lactone carbon some upfield shifted (Fig. S1). These spectra indicate that the cyanide anion was indeed added to the carbon of trifluoroacetyl group of **1**. The formation of cyanide adduct was further confirmed by mass spectrometry. The electrospray ionization mass spectrum of the probe **1** showed two molecular masses of 377.5 and 619.2, which corresponded to the formulas of [**1**-CN^-+HCN] and [**1**-CN^-+Bu_4NCN], respectively (Fig. 5b).[44,51]

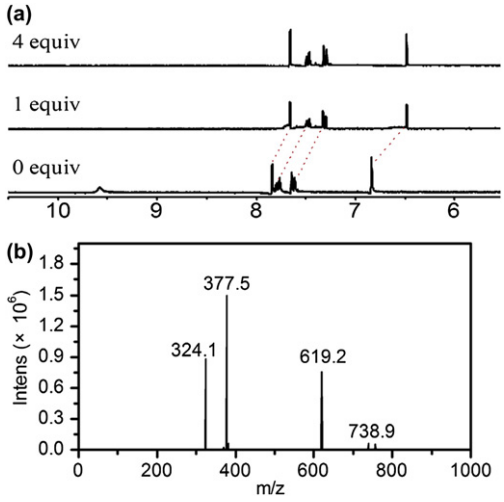

Fig. 5. (a) ^{1}H NMR spectral change of **1** in acetonitrile-d_3 upon addition of cyanide anions; (b) ESIMS for the cyanide adduct of **1**.

2.3. Quantum chemistry calculation

To understand the absorption and fluorescence changes of the probe **1** bound by cyanide ions we carried out density functional theory (DFT) and time dependent DFT (TDDFT) calculations with 6-31+G(d,p) basis sets (details see Supplementary data). The stable equilibrium structures of probe **1** and adduct **1**-CN^- were obtained from both B3LYP and PBE0 calculations, and the PBE0/6-31+G(d,p) geometry were shown in Fig. 6. The calculated N–H···O bond lengths of adduct **1**-CN^- are 2.226 and 2.250 Å in the ground state (S_0) and lowest excited state (S_1), respectively, which are typical intramolecular hydrogen bond. Fig. S2 shows simulated absorption spectra of probe **1** and adduct **1**-CN^- by TD-PBE0 and TD-B3LYP methods. Both results reproduce well the experimental data. As noted in Table S3, the CPCM-PBE0/6-31+G(d,p) calculated λ_{max} of probe **1** and adduct **1**-CN^- are 322 and 373 nm, which are slightly underestimated and overestimated, respectively, but in good agreement with experiment. The calculated HOMO–LUMO energy gaps of probe **1** and adduct **1**-CN^- are 4.50 and 3.89 eV, respectively (Fig. 7). As a result, experimental 329 nm absorption band of probe **1** red-shifts to 365 nm of adduct **1**-CN^- could be explained by the raise of HOMO energy level and enhancement in the push–pull character of the ICT transition. The Kohn Sham orbitals that are relevant to the excitations and the contributions of orbital transitions for probe **1** and adduct **1**-CN^- are given in Fig. S3. The electron density of the lowest unoccupied orbital (LUMO) of adduct **1**-CN^- is distributed more locally on the lactone ring of coumarin, while that of LUMO of probe **1** is delocalized on the entire coumarin through the trifluoroacetyl group. So the intramolecular charge at the first excited state of adduct **1**-CN^- is more obvious than that of probe **1**. More unambiguous, comparing charge difference densities between starting material **2**, probe **1**, and adduct **1**-CN^- in S_1 excitation were shown in Fig. 8. One can find that cyanohydrin formation and intramolecular hydrogen bonding results in enhancing intermolecular charge transfer. Similarly, fluorescence enhancement of cyanide ions adduct **1**-CN^- can also be explained by localization of the frontier orbitals in S_1 state (Fig. S3 and Table S3).

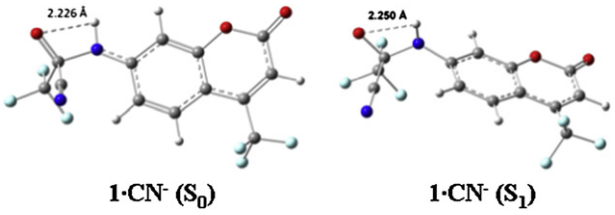

Fig. 6. The optimized structures of 1-CN^{-1} (left: the ground state; right: the lowest singlet state) with PBE0/6-31+G(d,p) method.

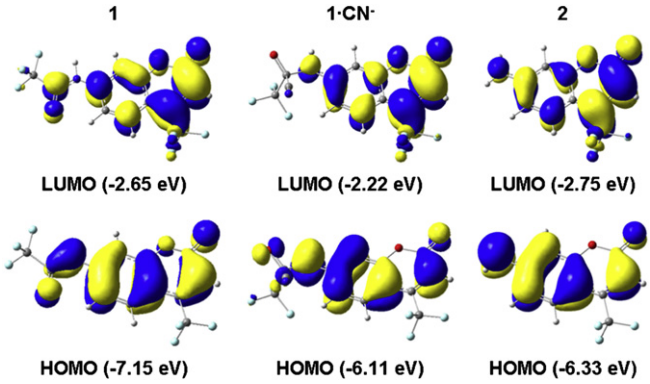

Fig. 7. Plot of Kohn Sham orbitals in ground state (S_0) for **2**, **1**, and **1**-CN^- (isovalue is 0.03 a.u) with CPCM-PBE0/6-31+G(d,p) method in acetonitrile solvent.

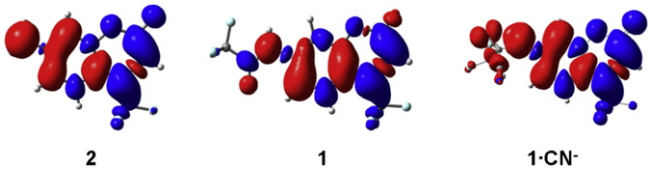

Fig. 8. Charge difference density of S_1 state for **2**, **1**, and **1**-CN^-. Red and blue stand for hole and electron, respectively. The isovalue is 0.0004 a.u.

2.4. Applications

As a probe for the assigned anion, response time is of importance to practical detection of analytes. The signaling of CN^- ions by probe **1** was very fast, which was complete really in less than 30 s (Fig. 9). As can be easily understood, the signaling time was concentration dependent, and the required time for full signaling increased considerably with lower CN^- concentrations (20 μM). On the other hand, the fluorescence intensity of probe **1** alone or in the

presence of a interference ions (F^-) remained nearly constant, even after 30 min of sample preparation. As a consequence, the nucleophilic addition of CN^- to carbonyl of probe **1** is an immediate response, thus providing a new realtime method for cyanide detection.

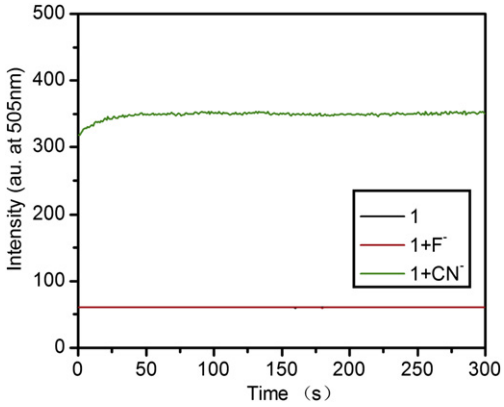

Fig. 9. Fluorescence intensity changes at 505 nm for **1** (20 μM, 25 °C) in a mixtures of CH_3CN/H_2O (4/1) after addition of CN^- and F^- (1 equiv). The excitation wavelength for the complex was 388 nm, and the splits were 5 nm.

The detection limit of probe **1** for CN^- was calculated based on the absorbance and fluorescence titration data according to a reported method.[43] Under the present conditions, a good linear relationship between the absorbance/the intensity and the cyanide concentration could be obtained, as shown in Fig. 10 and Fig. S4. The detection limits are then calculated with the equation: detection limit=3δ/m, where δ is the standard deviation of blank measurements, m is the slope between intensity versus sample concentration. The detection limits were measured to be 1.18 μM from absorption assay and 0.29 μM from fluorescent assay, respectively. The concentration limits are much lower than the limit (2 μM) set by Environment Protection Agency for drinking water.[13,52] Thus, this probe could be used for checking CN^- in drinking water following standard international norm. In order to assess the utility of the proposed method, it was applied to the quantitative determination of cyanide anion in drinking water sample (drinking water from commercial source). The water sample was found to be free from cyanide and so the sample was prepared by adding known amounts of sodium cyanide to sample. The applications were performed using 2 mL of sample volume, and after addition of sodium cyanide with the concentration of 9.8×10^{-7} M, which was within the linear calibration range, the sample was injected in triplicate. The average content of cyanide anion was found to be 9.99×10^{-7} M for drinking water. Then, the recovery percentage performed well with relative standard deviation lower than 2%.

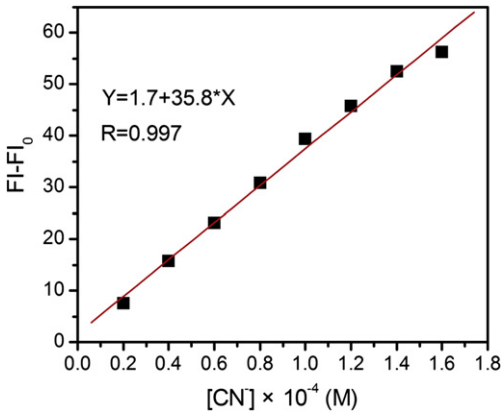

Fig. 10. A plot of ($FI-FI_0$) versus cyanide concentrations at 505 nm, the excitation wavelength for the complex was 388 nm, and the splits were 3 nm in CH_3CN/H_2O (4:1, v/v).

3. Conclusion

In summary, this investigation has led to the development of a rapid response and highly selective cyanide probe for detecting micromolar concentrations of CN^- ions in water. A unique colorimetric and fluorescent response to cyanide is realized through an early-reported mode of probe-cyanide interaction by formation of adduct cyanohydrin via a highly electron-deficient amide moiety in an aqueous environment. DFT/TDDFT calculations indicate that upon the addition of CN^- the fluorescence enhancement of probe **1** is mainly due to the ICT process improvement. The present probe **1** able to function as a selective and sensitive dual chromogenic and 'turn-on' fluorogenic chemosensor for the CN^-, whose response time is faster than those of the other trifluoroacetamide-based cyanide probes. The detection limit of the fluorescent assay for cyanide is as low as 0.3 μM in a fast response of less than 30 s and can be detected by the naked eyes, providing a new, realtime method for cyanide detection in the aqueous environment.

4. Experimental

4.1. Materials and apparatus

Commercially available compounds were used without further purification. Solvents were dried according to standard procedures. 7-Amino-4-trifluoromethylcoumarin was synthesized according to the reported procedure.[53] All reactions were magnetically stirred and monitored by thin-layer chromatography (TLC) using QingDao GF254 silica gel coated plates. Fluorescence spectra were carried out on a Shimadzu RF-5301PC fluorescence spectrophotometer. UV–vis spectra were recorded with a Shimadzu UV–2550 spectrophotometer. NMR spectra were recorded on a Bruker AV-300 Spectrometer (300 MHz for ^1H and 75 MHz for ^{13}C), and chemical shifts were referenced relative to tetramethylsilane (δ_H/δ_C=0). MALDI-TOF mass data were obtained by a Shimadzu AXIMA-CFR™ plus mass spectrometry, using a 1,8,9-anthracenetriol (DITH) matrix. ESIMS were taken on a Bruker-HCT mass spectrometer. X-ray diffraction experiment was performed with a Rigaku/MSC mercury diffractometer with graphite monochromated Mo Kα radiation (λ=0.71073 Å) at 293 K.

4.2. Preparation of probe 1

A solution of 7-amino-4-trifluoromethylcoumarin (60 mg, 0.26 mmol) and trifluoroacetic anhydride (116 mg, 0.78 mmol) was stirred in THF (5.5 mL) at room temperature for 1 h. Then the mixture was concentrated and purified by column chromatography eluted with ethyl acetate/petroleum ether (1:5) to afford the target compound **1** (76 mg) as pale yellow solid (R_f=0.2). The solid was recrystallized from $CHCl_3$ to give **1** as white needle crystal (69 mg), yield 80%. Mp: 182–184 °C; Found: C, 44.34; H, 1.50; N, 4.25$C_{12}H_5F_6NO_3$ requires C, 44.32; H, 1.55; N, 4.31%; ^1H NMR (300 MHz, acetone-d_6, ppm) δ: 10.81 (br, 1H, NH), 7.96 (d, J=1.80 Hz, 1H, ArH), 7.77–7.85 (m, 2H, ArH), 6.90 (d, J=0.6 Hz, 1H, ArH); ^{13}C NMR (75 MHz, acetone-d_6, ppm) δ: 158.0, 155.3 (q, J=38.1 Hz, $COCF_3$), 155.0, 140.7, 139.8 (q, J=32.6 Hz, =CCF_3), 125.8 (q, J=2.0 Hz, C=CCF_3), 121.8 (q, J=273.3 Hz, =CCF_3), 117.1, 115.8 (q, J=5.25 Hz, C=CCF_3), 115.7 (q, J=286.1 Hz, =CCF_3), 110.7, 108.6; MALDI-TOF Ms m/z: 326.50 $[M+1]^+$.

4.3. Spectral titration experiment of 1

Deionized water and a spectroscopic grade of CH_3CN were used as the solvent for titration experiment. The titrations were carried out in 10-mm quartz cuvettes at 25 °C. Probe **1** was dissolved in CH_3CN/H_2O (4:1, v/v) to afford a concentration of 5×10^{-4} M stock solution, which was diluted to 2×10^{-5} M. The different anion stock solutions of 1.0×10^{-2} M was diluted to 2.5×10^{-3} M. The absorbance was measured from 200 to 500 nm, against a blank CH_3CN/H_2O (4:1, v/v) solution, and different cyanide solutions were added to the 20 μM host solution (2 mL) in portions (total volume: 16, 32, 48, 64, 80, 96, 112, 128, 144, 160, 192, 224, 256, 288, 320, 480, 640, 800 μL of 2.5×10^{-3} M). The emission was measured from 425 to 625 nm, and different cyanide solutions were added to the 20 μM host solution (2 mL) in portions (total volume: 16, 32, 48, 64, 80, 96, 112, 128, 144, 160, 192, 224, 256, 288, 320, 400, 480, 640, 800, 960, 1120, 1280 μL of 2.5×10^{-3} M). The resulting solution was shaken well; the absorption and emission spectra were recorded immediately. Unless otherwise noted, for all measurements, the excitation wavelength was at 388 nm, and both the excitation and emission slit widths were 3 nm.

4.4. General procedure for ^{1}H NMR experiments

For ^{1}H NMR titrations, two stock solutions were prepared in acetonitrile-d_3 (5×10^{-2} M), one of them containing host only and the second one containing an appropriate concentration of guest. Aliquots of the two solutions were mixed directly in NMR tubes, which then was diluted to 0.5 mL with acetonitrile-d_3 if need be.

4.5. X-ray crystal structure determination of 1

X-ray diffraction experiment was performed with a Rigaku/MSC mercury diffractometer with graphite monochromated Mo Kα radiation (λ=0.71073 Å) at 293 K. Empirical absorption corrections based on equivalent reflections were applied. The crystal structure of **1** was solved by direct method and refined by full matrix least squares fitting on F^2 using the SHELXTL-97 software. All non-hydrogen atoms were refined with anisotropic thermal parameters. Crystallography data has been deposited to the Cambridge Crystallography Data Center with deposition number of 805,027 for **1**.

Acknowledgements

The authors acknowledge financial support from the National Natural Science Foundation of China (grant No.21062022), the Specialized Research Fund for the Doctoral Program of Higher Education (Grant No. 20102201110001) and the Opening Project of Key Laboratory for Chemistry of Low-Dimensional Materials of Jiangsu Province (No. JSKC10082).

Supplementary data

Supplementary data associated with this article can be found, in the online version, at doi:10.1016/j.tet.2011.07.023.

References and notes

1. Bianchi, A.; Bowman-James, K.; Garcia-Espána, E. *Supramolecular Chemistry of Anions*; Wiley-VCH: New York, NY, USA, 1997.
2. Timofeyenko, Y. G.; Rosentreter, J. J.; Mayo, S. *Anal. Chem.* **2007**, *79*, 251–255.
3. Vennesland, B.; Comm, E. E.; Knownles, C. J.; Westly, J.; Wissing, F. *Cyanide in Biology*; Academic: London, 1981.
4. Young, C.; Tidwell, L.; Anderson, C. *Cyanide: Social, Industrial, and Economic Aspects, Minerals, Metals, and Materials Society*; Warrendale: 2001.
5. Xu, Z.; Chen, X.; Kim, H. N.; Yoon, J. *Chem. Soc. Rev.* **2010**, *39*, 127–137.
6. Cho, D.-G.; Sessler, J. L. *Chem. Soc. Rev.* **2009**, *38*, 1647–1662.
7. Kim, Y.-H.; Hong, J.-I. *Chem. Commun.* **2002**, 512–513.
8. Liu, H.; Shao, X.-B.; Jia, M.-X.; Jiang, X.-K.; Li, Z.-T.; Chen, G.-J. *Tetrahedron* **2005**, *61*, 8095–8100.
9. Chow, C.-F.; Lam, M. H. W.; Wong, W.-Y. *Inorg. Chem.* **2004**, *43*, 8387–8393.
10. Zelder, F. H. *Inorg. Chem.* **2008**, *47*, 1264–1266.
11. Zeng, Q.; Cai, P.; Li, Z.; Qin, J.; Tang, B. Z. *Chem. Commun.* **2008**, 1094–1096.
12. Badugu, R.; Lakowicz, J. R.; Geddes, C. D. *J. Am. Chem. Soc.* **2005**, *127*, 3635–3641.
13. Ros-Lis, J. V.; Martínez-Máñez, R.; Sato, J. *Chem. Commun.* **2005**, 5260–5262.
14. Jin, W. J.; Fernández-Argüelles, M. T.; Costa-Fernández, J. M. *Chem. Commun.* **2005**, 883–885.
15. Touceda-Varela, A.; Stevenson, E. I.; Galve-Gasión, J. A.; Dryden, D. T. F.; Mareque-Rivas, J. C. *Chem. Commun.* **2008**, 1998–2000.
16. Chung, Y.; Lee, H.; Ahn, K. H. *J. Org. Chem.* **2006**, *71*, 9470–9474.
17. Sun, S. S.; Lees, A. J. *Chem. Commun.* **2000**, 1687–1688.
18. Miyaji, H.; Sessler, J. L. *Angew. Chem., Int. Ed.* **2001**, *40*, 154–157.
19. Saha, S.; Ghosh, A.; Mahato, P.; Mishra, S.; Mishra, S. K.; Suresh, E.; Das, S.; Das, A. *Org. Lett.* **2010**, *12*, 3406–3409.
20. Gimeno, N.; Li, X.; Durrant, J. R.; Vilar, R. *Chem.—Eur. J.* **2008**, *14*, 3006–3012.
21. Anzenbacher, P., Jr.; Tyson, D. S.; Jursíková, K.; Castellano, F. N. *J. Am. Chem. Soc.* **2002**, *124*, 6232–6233.
22. Tomasulo, M.; Sortino, S.; White, A. J. P.; Raymo, F. M. *J. Org. Chem.* **2006**, *71*, 744–753.
23. Ren, J. Q.; Zhu, W. H.; Tian, H. *Talanta* **2008**, *75*, 760–764.
24. Tomasulo, M.; Raymo, F. M. *Org. Lett.* **2005**, *7*, 4633–4636.
25. Garcia, F.; Garcia, J. M.; Garcia-Acosta, B.; Martinez-Manez, R.; Sancenon, F.; Soto, J. *Chem. Commun.* **2005**, 2790–2792.
26. Ros-Lis, J. V.; Martínez-Máñez, R.; Sato, J. *Chem. Commun.* **2002**, 2248–2249.
27. Yang, Y. K.; Tae, J. *Org. Lett.* **2006**, *8*, 5721–5723.
28. Lee, K. S.; Kim, S. H.; Kim, G. H.; Shin, I.; Hong, J. I. *Org. Lett.* **2008**, *10*, 49–51.
29. Kwon, S. K.; Kou, S.; Kim, H. N.; Chen, X. Q.; Wang, H.; Nam, S. W.; Kim, S. H.; Swamy, K. M. K.; Park, S.; Yoon, J. *Tetrahedron Lett.* **2008**, *49*, 4102–4105.
30. Lee, K. S.; Lee, J. T.; Hong, J.-I.; Kim, H.-J. *Chem. Lett.* **2007**, *36*, 816–817.
31. Kim, Y. K.; Lee, Y.-H.; Lee, H.-Y.; Kim, M. K.; Cha, G. S.; Ahn, K. H. *Org. Lett.* **2003**, *5*, 4003–4006.
32. Chung, Y. M.; Raman, B.; Kim, D.-S.; Ahn, K. H. *Chem. Commun.* **2006**, 186–188.
33. Ryu, D.; Park, E.; Kim, D.-S.; Yan, S.; Lee, J. Y.; Chang, B. Y.; Ahn, K. H. *J. Am. Chem. Soc.* **2008**, *130*, 2394–2395.
34. Kim, D.-S.; Chung, Y.-M.; Jun, M.; Ahn, K. H. *J. Org. Chem.* **2009**, *74*, 4849–4854.
35. Kim, D.-S.; Ahn, K. H. *J. Org. Chem.* **2008**, *73*, 6831–6834.
36. Niu, H. T.; Jiang, X. L.; He, J. Q.; Cheng, J. P. *Tetrahedron Lett.* **2008**, *49*, 6521–6524.
37. Niu, H. T.; Su, D.; Jiang, X.; Yang, W.; Yin, Z.; He, J.; Cheng, J. P. *Org. Biomol. Chem.* **2008**, *6*, 3038–3040.
38. Ekmekci, Z.; Yilmaz, M. D.; Akkaya, E. U. *Org. Lett.* **2008**, *10*, 461–464.
39. Yu, H. B.; Zhao, Q.; Jiang, Z. X.; Qin, J. G.; Li, Z. *Sens. Actuators, B* **2010**, *148*, 110–116.
40. Peng, L. H.; Wang, M.; Zhang, G. X.; Zhang, D. Q.; Zhu, D. B. *Org. Lett.* **2009**, *11*, 1943–1946.
41. Sessler, J. L.; Cho, D.-G. *Org. Lett.* **2008**, *10*, 73–75.
42. Miyaji, H.; Kim, D.-S.; Chang, B.-Y.; Park, E.; Park, S.-M.; Ahn, K. H. *Chem. Commun.* **2008**, 753–755.
43. Sun, Y.; Liu, Y. L.; Chen, M. L.; Guo, W. *Talanta* **2009**, *80*, 996–1000.
44. Sun, Y.; Liu, Y. L.; Guo, W. *Sens. Actuators, B* **2009**, *143*, 171–176.
45. Cho, D.-G.; Kim, J. H.; Sessler, J. L. *J. Am. Chem. Soc.* **2008**, *130*, 12163–12167.
46. Kim, H. J.; Ko, K. C.; Lee, J. H.; Lee, J. Y.; Kim, J. S. *Chem. Commun.* **2011**, 2886–2888.
47. Saxena, J. P.; Stafford, W. H.; Stafford, W. L. *J. Chem. Soc., Chem. Commun.* **1959**, 1579–1587.
48. Benesi, H. A.; Hildebrand, J. H. *J. Am. Chem. Soc.* **1949**, *71*, 2703–2707.
49. Nevado, J. J. B.; Pulgarin, J. A. M.; Laguna, M. A. G. *Talanta* **2001**, *53*, 951–959.
50. Yu, T. Z.; Zhao, Y. L.; Fan, D. W. *J. Mol. Struct.* **2006**, *791*, 18–22.
51. Chen, C.-L.; Chen, Y.-H.; Chen, C.-Y.; Sun, S.-S. *Org. Lett.* **2006**, *8*, 5053–5056.
52. http://www.epa.gov/safewater/contaminants/index.html.
53. Bissell, E. R.; Mitchell, A. R.; Smith, R. E. *J. Org. Chem.* **1980**, *45*, 2283–2287.